Comparison of Nickel-Group Metal Cyanides and Acetylides and Their Anions Using Anion Photoelectron Spectroscopy and Density Functional Theory Calculations

Bappaditya Chatterjee,[†] F. Ahu Akin,[‡] Caroline Chick Jarrold,* and Krishnan Raghavachari

Indiana University, Department of Chemistry, 800 East Kirkwood Avenue, Bloomington, Indiana 47405-7102

Received: April 21, 2005; In Final Form: June 15, 2005

The photoelectron spectra of $NiCN^-$, $PdCN^-$, $PtCN^-$, $HNiC_2H^-$, $Ni(C_2H)_2^-$, PdC_2H^-, and PtC_2H^- are presented along with density functional theory calculations. Linear structures are predicted for all anions and neutrals. $NiCN^-$ and NiCN are predicted to have $^3\Delta$ and $^2\Delta$ ground states, respectively. $HNiC_2H^-$ and $Ni(C_2H)_2^-$ are predicted to have $^2\Delta$ and $^2\Delta_g$ anion and $^3\Delta$ and $^3\Pi_g$ neutral ground states, respectively. The palladium and platinum cyanide and acetylides have $^1\Sigma^+$ anion and $^2\Sigma^+$ neutral ground states. Simulations generated from the calculated parameters are compared to observed spectra, and molecular orbital diagrams are presented to compare the bonding in these species.

I. Introduction

Simple, metal atom-based complexes are of broad interest for reasons ranging from their catalytic[1,2] to interstellar[3] relevance. Transition metal cyanides are a well-studied class of compounds.[4,5] Gas-phase unsaturated metal cyanides have been receiving a steady stream of theoretical and experimental attention because of the variety of isomers that may form (M−CN and M−NC, along with T-shaped structures). A paper by Kingston et al.[6] reporting the laser-induced fluorescence of NiCN provides an excellent summary of more recent studies on a number of metal cyanides and their various structures. Metal alkynyl complexes have also come under scrutiny motivated by their potential in the development of new molecular electronic systems,[7] nonlinear optical materials,[8,9] and luminescent materials.[10] Ni and Pd diimines have received theoretical[11] and experimental[12−14] attention for their catalytic role in ethylene polymerization. Pd nanoparticles have been investigated for the application of acetylene polymerization,[15] and there have been theoretical studies of acetylene interaction with group 10 surfaces[16] including a study on the hydrogenation of acetylene on Pd.[17]

The nature of bonding in unsaturated metal cyanides and acetylides is therefore of some interest. In this paper, we report density functional theory (DFT) calculations and anion photoelectron (PE) spectra of a series of group 10 cyanide and acetylide complexes, as a continuation of previous studies on unsaturated group 10 metal complexes formed in gas-phase reactions.[18−20] The predominantly ionic cyanide and acetylide complexes discussed in this paper show both similarities and fundamental differences in bonding with the carbonyls studied previously.[20]

II. Methods

Experimental Details. The apparatus used in these experiments has been described elsewhere.[18,19,21] Briefly, the cyanide complex ions are generated using a laser ablation/pulsed molecular beam valve source. A metal target is ablated with approximately 10 mJ/pulse of 532 nm (doubled) output of a Nd:YAG laser operating at a 30 Hz repetition rate, and the resulting plasma is entrained in the output of a solenoid-type molecular beam valve backed by 80 psig He/acetonitrile (ambient vapor pressure). The MCN^- species are formed by association of a neutral metal atom and CN^-. The complexes cool in a 2 cm long, 3 mm diameter clustering channel, then expand into the vacuum. The nickel acetylide complexes were similarly generated, with 80 psi, 1% C_2H_4/balance He carrier gas. PdC_2H^- and PtC_2H^- were generated with a pure He carrier gas, and a second valve was coupled to the clustering channel to introduce ethylene (1% in a 80 psi mixture with He) downstream of the ablation site.

After expanding from the clustering channel, the anions pass through a 3 mm skimmer, and are accelerated to 1 keV into a 1.2-m beam modulated time-of-flight mass spectrometer. Prior to colliding with an ion detector, the anions of interest are selectively photodetached using the third harmonic output (355 nm, 3.49 eV) of a second Nd:YAG laser at the intersection of the ion beam and a second, 1-m field-free drift tube situated perpendicular to the ion beam. A small fraction (10^{-4}) of the photoelectrons that travel up the center of the second drift tube collides with a dual microchannel plate detector. The electron drift times are recorded with a digitizing oscilloscope. The spectra below were signal averaged from 120000 to 400000 laser shots. The drift times of the photoelectrons are converted to binding energy ($BE = h\nu - e^-KE$) binned into 2 meV intervals. The apparatus is calibrated frequently during data acquisition by obtaining the PE spectra of I^-, O^-, OH^-, Ni^-, Pd^- and Pt^-, all of which have well-known EAs. Spectra are collected with the electric field vector of the laser both parallel and perpendicular to the direction of electron detection for all species. Except for PdC_2H^- [18] and $NiC_2H_2^-$, peak intensities changed fairly uniformly with respect to polarization.

Computational Details. Geometry optimizations and vibrational calculations were done using the Gaussian 98 program package.[22] DFT calculations with the B3LYP functional (three-parameter hybrid Becke exchange and Lee−Yang−Parr correlation)[23] were performed on a number of electronic states of

* Corresponding author. E-mail: cjarrold@indiana.edu.
[†] Current address: RD&E Phillip Morris USA, 4201 Commerce Road, Richmond, VA, 23234.
[‡] Current address: University of Arizona, Department of Chemistry, 1306 East University Blvd., Tucson, AZ 85721.

10.1021/jp0520704 CCC: $30.25
Published on Web 07/20/2005

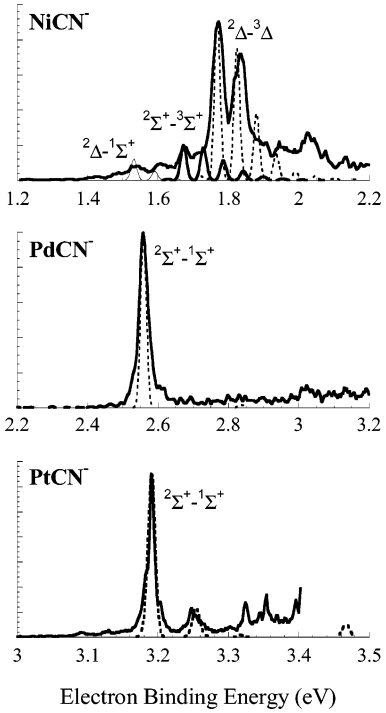

Figure 1. 3.49 eV PE spectra (solid lines) and simulations of spectral profiles based on the calculated structural parameters for (a) $NiCN^-$/NiCN, (b) $PdCN^-$/PdCN, and (c) $PtCN^-$/PtCN. Note that in the case of multiplet states, simulation of only one spin−orbit component is shown.

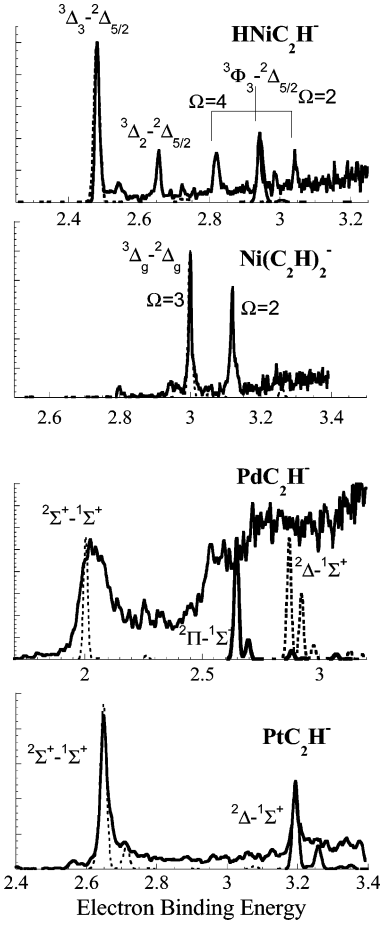

Figure 2. 3.49 eV PE spectra (solid lines) and simulations of spectral profiles based on the calculated spectroscopic parameters for (a) $HNiC_2H^-$, (b) $Ni(C_2H)_2^-$, (c) PdC_2H^-, and (d) PtC_2H^-. Note that in the case of multiplet states, simulation of only one spin−orbit component is shown.

the anion and neutral cyanide and acetylide complexes, as well as the anion and neutral isocyanide (M−NC) complexes (T-shaped structures converged to linear structures). For the nickel acetylide complexes, a number of geometries were attempted, but the linear, divalent structures were the most stable. For the NiCN anion and neutral, the 6-311+G(2d,p) basis set[22] was used. This basis set contains diffuse (s, p) and polarization (two sets of d) functions on C and N and diffuse (s, two sets of p, d) and polarization (two sets of f) functions on Ni. For the $HNiC_2H$ and $Ni(C_2H)_2$ anion and neutrals, the 6-311+G(df,p) basis set[22] was used. This basis set contains diffuse (s, p) and polarization (d, f) functions on C and diffuse (s, two sets of p, d) and polarization (f, g) functions on Ni. For all the Pd and Pt complexes, the LANL2DZ basis set augmented with s, p, d, and two sets of f functions was used on the metal atom, and the 6-311+G(2d,p) basis set was used for the C, N, and H atoms.

III. Results and Analysis

Spectra of the cyanide and acetylide complexes are shown as solid traces in Figures 1 and 2, respectively. Note that the spectra are shown on different energy scales. The results of the calculations on all the species, anions and neutrals, plus multiple excited states, are summarized in Tables 1−7. On the basis of the calculated anion and neutral structures, normal coordinates and vibrational frequencies, simulations were performed making (1) Born−Oppenheimer, (2) parallel mode, and (3) harmonic oscillator approximations. These simulations are shown as dashed or gray lines superimposed on the spectra. Since no spin−orbit effects were included in the calculations, only one spin−orbit component is included in the simulation of multiplet neutral states. Band assignments shown on the spectra are based on the calculated states, as discussed below.

A. Cyanide Complexes. $NiCN^-$. The results of the DFT calculations on NiCN and $NiCN^-$, summarized in Table 1, predict that cyanide (Ni−C−N) structures are energetically favored over the isocyanide structures (Ni−N−C) for both the anion and neutral. A $^3\Delta$ [...$(2\pi)^4(4\sigma)^2(1\delta)^3(5\sigma)$] ground state is predicted for $NiCN^-$, with close-lying $^3\Sigma^+$[...$(4\sigma)(1\delta)^4(5\sigma)$], $^1\Sigma^+$-[...$(4\sigma)^2(1\delta)^4$] and $^3\Pi$ [...$(2\pi)^3(4\sigma)^2(1\delta)^4(5\sigma)$] states. Other triplet states were found much higher in energy. A $^2\Delta$ [...$(4\sigma)^2(1\delta)^3$] ground and $^2\Sigma^+$ [...$(4\sigma)(1\delta)^4$] and $^2\Pi$ [...$(2\pi)^3(4\sigma)^2(1\delta)^4$] low-lying excited states are predicted for the neutral. The $\tilde{X}_1{}^2\Delta_{5/2}$, $\tilde{X}_2{}^2\Delta_{3/2}$, and $\tilde{W}_1{}^2\Pi_{3/2}$ states were previously investigated by laser-induced fluorescence.[6] The term energy of the $\tilde{W}_1{}^2\Pi_{3/2}$ state is 2238 cm^{-1} (0.277 eV) which is in reasonable agreement with the 0.20 eV (unperturbed) value calculated here.

Of the three neutral states, only the $^2\Delta$ neutral state is accessible via a one-electron transition from the $^3\Delta$ anion ground state, based on the zero-order orbital occupancies. The $^3\Delta$ state emerges definitively as the anion ground state and the neutral ground state is known to be $^2\Delta_{5/2}$,[6] suggesting the $^2\Delta_{5/2}-{}^3\Delta_3$ assignment of the band originating at 1.771(10) eV in the PES (Figure 1, top panel). The calculated EA of NiCN is 1.56 eV, 0.21 eV lower than observed (spin−orbit splittings from ∼500 to 1500 cm^{-1} are anticipated for multiplet states[27] in *both* the anion and neutral moiety).

The second most prominent peak in this band is spaced by 470(50) cm^{-1} from the origin. The Ni−CN stretch for the ground neutral state is calculated to be 477 cm^{-1}, while the $^2\Delta_{5/2}-{}^2\Delta_{3/2}$ splitting was determined to be 830 cm^{-1}.[6] This therefore is a vibrational overtone. As shown by the simulation (only one spin−orbit component shown), which has been shifted

TABLE 1: Summary of DFT Calculations [B3LYP/6-311+G(2d,p)] on NiCN, $NiCN^-$, and the Ground Energy States of the Isocyanide Structural Isomers

state	energy (hartree)	relative energy (eV)	R_{Ni-C} R_{C-N} (Å)	vibrational frequencies (cm^{-1})
		NiCN		
$^2\Pi$	−1601.15280	1.76	1.888	2229 (σ)
			1.158	450 (σ)
				224, 241 (π)
$^2\Sigma^+$	−1601.14969	1.57	1.869	2235 (σ)
			1.158	458 (σ)
				246 (π)
$^2\Delta$	−1601.15015	1.56	1.850	2241 (σ)
		exptl EA = 1.771(10)	1.158	477 (σ)
				249 (π)
		$NiCN^-$		
$^3\Phi$	−1601.13143	2.07		
$^3\Sigma^-$	−1601.13619	1.94		
$^3\Pi$	−1601.20143	0.16	1.987	2186 (σ)
			1.164	352 (σ)
				213, 223 (π)
$^1\Sigma^+$	−1601.20245	0.14	1.788	2133 (σ)
			1.169	485 (σ)
				319 (π)
$^3\Sigma^+$	−1601.20454	0.08	1.956	2172 (σ)
			1.165	357 (σ)
				206 (π)
$^3\Delta$	−1601.20740	0	1.937	2179 (σ)
			1.165	376 (σ)
				225 (π)
		NiNC		
$^2\Delta$	−1601.13182	2.06		
$^2\Sigma^+$	−1601.13448	1.98		
		(EA = 1.71)		
		$NiNC^-$		
$^3\Delta$	−1601.19751	0.27		

to match the observed origin, the calculations predict a fair amount of excitation of the Ni−CN stretch, but virtually no activation of the C−N stretch, which would have coincided with 2.026 eV in the experimental spectrum. There is no evidence for the $^2\Delta_{3/2}-{}^3\Delta_3$ transition 830 cm^{-1} (0.103 eV) above the origin, except possibly the 1.874 eV shoulder, suggesting that the photoelectron has predominantly p-wave character. The detachment nominally involves the 5σ orbital (Ni 4s hybridized with lesser amounts of $4p_z$ and $3d_{z^2}$). In this case, the $\Omega = {}^5/_2$ neutral level should be favored over the ${}^3/_2$ level by the $\Omega = 3$ anion level (the $\Omega = 2$ level of the anion could access both the $\Omega = {}^5/_2$ and ${}^3/_2$ neutral levels, while the $\Omega = 1$ level would favor the $\Omega = {}^3/_2$ neutral level).[28]

Structures observed at 1.675(10) and 1.534(10) eV, because of their energy relative to the origin [1.771(10) eV] appear to be electronic (rather than vibrational) hot bands. The spectral assignments shown on the spectrum are most consistent with the calculated term energies of the various states, bearing in mind the 1-e^- transition propensity rule (from $^3\Sigma^+$ anion state, only the $^2\Sigma^+$ neutral state can be accessed; all three neutral states can be accessed from the $^1\Sigma^+$ anion state).

$PdCN^-$. The PE spectrum of $PdCN^-$ (Figure 1, center panel) as previously discussed,[19] shows a single, narrow electronic transition at 2.543(7) eV, and assigned to the $^2\Sigma^+-{}^1\Sigma^+$ transition. Consistent with the spectral profile, the calculations, summarized in Table 2, predict similar structures for the anion and neutral, having $^1\Sigma^+$ [...$(2\pi)^4(1\delta)^4(4\sigma)^2$] and $^2\Sigma^+$ [...$(2\pi)^4(1\delta)^4(4\sigma)$] ground states, respectively. The simulation bears this out. The calculated EA is 2.58 eV, which is in good agreement with experiment. The triplet manifold of $PdCN^-$ begins at T_e = 1.6 eV, which is not thermally accessible in the ion beam and would not contribute to the observed spectra. The change in Pd−C bond length between the anion and neutral ground states is predicted to be only 0.003 Å. The C−N bond length change is larger: 0.01 Å. The lowest-lying excited neutral states, $^2\Delta$ [...$(2\pi)^4(1\delta)^3(4\sigma)^2$] and $^2\Pi$ [...$(2\pi)^3(1\delta)^4(4\sigma)^2$] states, are calculated to lie just above 3.4 eV, which is above the experimental cutoff.

TABLE 2: Summary of DFT Calculations [B3LYP/LANL2DZ + (spd2f) on Pd and 6-311+G(2d,p) on C and N] for PdCN, $PdCN^-$ and Ground States of the Isocyanide Isomers

state	energy (hartree)	relative energy (eV)	R_{Pd-C} R_{C-N} (Å)	vibrational frequencies (cm^{-1})
		PdCN		
$^2\Pi$	−219.55635	3.43	2.020	2111 (σ)
			1.166	378 (σ)
				181; 218 (π)
$^2\Delta$	−219.55667	3.42	2.022	2248 (σ)
			1.157	401 (σ)
				235 (π)
$^2\Sigma^+$	−219.58759	2.58	1.951	2228 (σ)
		exptl EA = 2.543(8)	1.158	433 (σ)
				266 (π)
		$PdCN^-$		
$^1\Sigma^+$	−219.68242	0	1.948	2147 (σ)
			1.168	401 (σ)
				285 (π)
		PdNC		
$^2\Sigma^+$	−219.56170	3.29	1.961	2138 (σ)
		(EA = 2.56)	1.172	433 (σ)
				178 (π)
		$PdNC^-$		
$^1\Sigma^+$	−219.65582	0.72	2.007	2131 (σ)
			1.170	346 (σ)
				178 (π)

TABLE 3: Summary of DFT Calculations [B3LYP/LANL2DZ + (spd2f) on Pt and 6-311+G(2d,p) on C and N] for PtCN, $PtCN^-$, and Ground States of the Isocyanide Isomers

state	energy (hartree)	relative energy (eV)	R_{Pt-C} R_{C-N} (Å)	vibrational frequencies (cm^{-1})
		PtCN		
$^2\Pi$	−211.96857	3.72	1.882	2030 (σ)
			1.170	477 (σ)
				280; 319 (π)
$^2\Delta$	−211.98241	3.34	1.913	2253 (σ)
			1.157	503 (σ)
				311 (π)
$^2\Sigma^+$	−211.98622	3.24	1.897	2229 (σ)
		exptl EA = 3.191(5)	1.159	511 (σ)
				323 (π)
		$PtCN^-$		
$^1\Sigma^+$	−212.10532	0	1.860	2135 (σ)
			1.170	532 (σ)
				383 (π)
		PtNC		
$^2\Sigma^+$	−211.94561		1.899	2131 (σ)
		(EA = 3.19)	1.173	505 (σ)
				224 (π)
		$PtNC^-$		
$^1\Sigma^+$	−212.06266	1.16	1.879	2115 (σ)
			1.1702	507 (σ)
				282 (π)

$PtCN^-$. The DFT calculations on $PtCN^-$ and PtCN, summarized in Table 3, predict $^1\Sigma^+$ and $^2\Sigma^+$ anion and neutral ground states, respectively, analogous to those obtained for $PdCN^-$ and PdCN. The triplet manifold of $PtCN^-$ lies above

TABLE 4: Results of DFT Calculations [B3LYP/6-311+G(df+p)] on $HNiC_2H$ and $HNiC_2H^-$

state	energy (hartree)	relative energy (eV)	R_{H-Ni}; R_{Ni-C} R_{C-C}; R_{C-H} (Å)	totally symmetric modes (cm^{-1})[a]
		HNiCCH		
$^3\Phi$	−1585.59456	3.28	1.566; 1.896	481, 1895
		exptl 2.986(5)	1.226; 1.067	1983, 3434
$^3\Sigma^-$	−1585.60152	3.09	1.591; 1.897	496; 1894
			1.224; 1.067	1997; 3437
$^3\Pi$	−1585.61545	2.71	1.557; 1.906	483, 1900
			1.220; 1.066	2028, 3440
$^3\Delta$	−1585.61892	2.61	1.529; 1.923	476, 1918
		exptl EA = 2.531(5)	1.214; 1.065	2087, 3449
		$HNiCCH^-$		
$^2\Sigma^+$	−1585.70522	0.26	1.609; 1.925	404, 1581
			1.229; 1.065	1983, 3432
$^2\Pi$	−1585.70774	0.20	1.590; 1.944	404, 1663
			1.226; 1.065	1995, 3434
$^2\Delta$	−1585.71493	0	1.558; 1.916	417, 1693
			1.227; 1.065	1991, 3435

[a] In order, they are nominally described as the $HNi-C_2H$ stretch, the $H-NiC_2H$ stretch, the HNiC−CH stretch, and the HNiCC−H stretch. Bend modes are not included for brevity.

TABLE 5: Results of DFT Calculations [B3LYP/6-311+G(df+p)] on $Ni(C_2H)_2$ and $Ni(C_2H)_2^-$

state	energy (hartree)	relative energy (eV)	R_{Ni-C} R_{C-C}; R_{C-H} (Å)	totally symmetric modes[41] (cm^{-1})[a]
		$Ni(C_2H)_2$		
$^3\Phi_g$	−1661.79618	3.47	1.877	423; 1999
			1.224; 1.066	3438
				R−T active
$^3\Sigma^-$	−1661.80638	3.19	1.883	425; 2006
			1.223; 1.066	3437
$^3\Delta_g$	−1661.80785	3.15	1.898	428; 2096
		exptl 3.000(5)	1.213; 1.065	3445
$^3\Pi_g$	−1661.81338	3.003	1.885	426; 2030
			1.219; 1.066	3442
				R−T active
		$Ni(C_2H)_2^-$		
$^2\Pi_g$	−1661.91674	0.19	1.923	370; 2010
			1.224; 1.065	3437
$^2\Sigma_g^+$	−1661.91772	0.16	1.915	370; 2004
			1.226; 1.065	3437
$^2\Delta_g$	−1661.92373	0	1.899	388; 2015
			1.225;1.065	3438

[a] In order, these are the in-phase $(HC_2)-Ni-(C_2H)$, the HC−CNiC−CH, and the $H-C_2NiC_2-H$ stretches. Bend modes are not included for brevity.

T_e = 1.48 eV. These are not thermally accessible in the ion beam and would not contribute to the observed spectra, and so they are not included in Table 3. The excited states of PtCN are predicted to be closer to the neutral ground state than the excited states of PdCN. The unperturbed binding energies of the $^2\Delta$ and $^2\Pi$ states are predicted to be 3.34 and 3.72 eV. Note, however, that the spin−orbit splittings (on the order of 1 eV) are comparable to the unperturbed term energies, so all spectral assignments should be treated as tentative.[29]

The PE spectrum of $PtCN^-$ (Figure 1, bottom panel) shows very narrow structure. The most prominent peak, assigned to the $^2\Sigma^+-{}^1\Sigma^+$ transition is at 3.191(3) eV (the adiabatic EA of PtCN), in good agreement with the calculated value, 3.24 eV. Note that the simulation suggests that the peak at 3.248 eV in the experimental spectrum is the fundamental of the Pt−CN stretch. Higher-lying structure found at 3.326(5) and 3.354(5) eV, respectively, are not accounted for by the $^2\Sigma^+-{}^1\Sigma^+$ simulation, and they are therefore two separate electronic transitions.

B. Acetylide Complexes. $NiC_2H_2^-$. Calculations on the neutral and anion structures of NiC_2H_2 predict linear H−Ni−C−C−H structures as being the most stable. As summarized in Table 4, $^2\Delta$ [...$(2\pi)^4(5\sigma)^2(1\delta)^3$] and $^3\Delta$ [...$(2\pi)^3(5\sigma)(1\delta)^3$] anion and neutral ground states are predicted, respectively. Two low-lying excited anion states, $^2\Pi$ [...$(2\pi)^3(5\sigma)^2(1\delta)^4$] and $^2\Sigma^+$ [...$(2\pi)^4(5\sigma)(1\delta)^4$] were also found. Four neutral states, three of which should show measurable spin−orbit splitting with our experiment, are predicted to lie within 3.3 eV of the ground anion state (or within 0.7 eV of the ground neutral state). On the basis of the one-electron transition propensity rule, the $^3\Delta$ and $^3\Phi$ [...$(2\pi)^3(5\sigma)^2(1\delta)^3$] neutral states can be accessed from the $^2\Delta$ anion ground state. The $^1\Sigma^+$ and $^3\Sigma^+$ excited neutral states (analogous to the lowest-lying excited states of $NiCN^-$) are predicted to lie above the experimental cutoff.

All prominent features in the spectrum (Figure 2, top panel) are assigned to the various spin−orbit components of the $^3\Delta-{}^2\Delta_{5/2}$ and $^3\Phi-{}^2\Delta_{5/2}$ transitions, and they are consistent with the following observations: (1) For the $^3\Delta-{}^2\Delta_{5/2}$ transition, we expect a $\Omega' = 3$ or $2 \leftarrow \Theta'' = {}^5/_2$ spin−orbit propensity rule to apply, assuming the σ orbital involved in the detachment has a dominant Ni 4s component. This does *not* apply to the $^3\Phi-{}^2\Delta_{5/2}$ transition, and all three $^3\Phi_{4,3,\text{and}2}$ components should be observed. (2) Simulations of both the $\Delta-\Delta$ and $\Phi-\Delta$ transitions are nearly vertical, so all relatively intense peaks are not from vibrational progressions. (3) In polarization studies (not shown), those peaks assigned as $\Delta-\Delta$ transitions show strong polarization dependence consistent with predominantly p-wave photoelectron character, while those assigned as $\Phi_{4,3}-\Delta$ transitions show no marked polarization dependence, consistent with *s*-wave character.[30] The $\Phi_2-\Delta$ did show similar polarization dependence with the ground-state peaks, but this may be associated with the lower kinetic energy of the electrons at this binding energy. (4) As shown in Table 4, there is good agreement between the calculated and observed transition energies, assuming these assignments.

$Ni(C_2H)_2^-$. The results of the DFT calculations on both $Ni(C_2H)_2^-$ and the neutral moiety predict that the linear, bivalent $D_{\infty h}$ structures are energetically favored over any lower-symmetry linear, bent, or cyclic structures. As summarized in Table 5, $Ni(C_2H)_2^-$ is predicted to have a $^2\Delta_g$ [...$(3\pi_g)^4(5\sigma_g)^2(1\delta_g)^3$] ground state, analogous to $HNiC_2H^-$. The $^2\Sigma_g^+$ [...$(3\pi_g)^4(5\sigma_g)(1\delta_g)^4$] and $^2\Pi_g$ [...$(3\pi_g)^3(5\sigma_g)^2(1\delta_g)^4$] excited anion states are predicted to lie within 0.2 eV, with their ordering reversed relative to $HNiC_2H^-$. In contrast to $HNiC_2H$, $Ni(C_2H)_2$ neutral is predicted to have a $^3\Pi_g$ [...$(3\pi_g)^3(5\sigma_g)(1\delta_g)^4$] ground state. The $^3\Delta_g$, $^3\Sigma_g^-$[...$(3\pi_g)^2(5\sigma_g)^2(1\delta_g)^4$], and $^3\Phi_g$ [...$(3\pi_g)^3(5\sigma_g)^2(1\delta_g)^3$] states are found within 0.5 eV of the ground neutral state. The $^3\Pi_g$ state is *not* accessible from the $^2\Delta_g$ anion state via a one-electron transition; only the $^3\Delta_g$ and $^3\Phi_g$ states are accessible from the $^2\Delta_g$ state (and only the $\Omega = 3$ and 2 components of the $^3\Delta_g$ state can be accessed from the $\Omega = {}^5/_2$ spin−orbit component of the $^2\Delta_g$ state), so we *cannot* determine the adiabatic EA of $Ni(C_2H)_2$ directly from the spectrum. The $^3\Pi_g$ state can be accessed from the excited $^2\Sigma_g^+$ anion state, which is calculated at 0.16 eV (1290 cm^{-1}) above the (unperturbed) ground anion state.

The PE spectrum of $Ni(C_2H)_2^-$ shown in Figure 2, second panel, exhibits two prominent peaks at 3.000(5) and 3.119(5) eV [960(60) cm^{-1} interval]. A much lower intensity peak at 2.797(5) eV lies 1640(60) cm^{-1} to lower binding energy. On the basis of the calculated states outlined above, the more intense structure is assigned to the $^3\Delta_g(3)-{}^2\Delta_g(5/2)$ and $^3\Delta_g(2)-{}^2\Delta_g(5/2)$ transitions, as indicated on the spectrum. A simulation of

TABLE 6: Results of DFT Calculations [B3LYP/LANL2DZ + (spd2f) on Pd and 6-311+G(2d,p) on C and H] on PdC_2H and PdC_2H^-

state	energy (hartree)	relative energy (eV)	R_{Pd-C} R_{C-C}; R_{C-H} (Å)	vibrational frequencies (cm^{-1})[a]
		PdCCH		
$^2\Delta$	−203.44488	2.87	2.004 1.209; 1.064	3444; 2084 424 652; 207
$^2\Pi$	−203.45299	2.65	1.963 1.228; 1.066	3426; 1897 411 705/568; 174/199
$^2\Sigma^+$	−203.47664	2.01 exptl EA = 1.98(3)	1.938 1.209; 1.064	3449;2089 453 619;229
		$PdCCH^-$		
$^1\Sigma^+$	−203.55035	0	1.932 1.225; 1.064	3435; 1984 421 479; 260

[a] In order, these are the PdC_2−H stretch, the PdC−CH stretch, the Pd−C_2H stretch, and then the two bend frequencies. The $^2\Pi$ state is Renner−Teller active; both bend components are included for both modes.

TABLE 7: Results of DFT Calculations [B3LYP/LANL2DZ + (spd2f) on Pt and 6-311+G(2d,p) on C and H] on PtC_2H and PtC_2H^-

state	energy (hartree)	relative energy (eV)	R_{Pt-C} R_{C-C}; R_{C-H} (Å)	vibrational frequencies (cm^{-1})[a]
		PtCCH		
$^2\Pi$	−195.87431	2.84	1.844 1.228; 1.065	3437; 1882 530 489/706; 321/391
$^2\Delta$	−195.87676	2.77	1.907 1.206; 1.063	3457; 2121 521 795; 636
$^2\Sigma^+$	−195.87950	2.70 exptl EA = 2.650(10)	1.894 1.207; 1.063	3458; 2110 526 580;249
		$PtCCH^-$		
$^1\Sigma^+$	−195.97854	0	1.856 1.224; 1.061	3460; 2008 545 414; 342

[a] In order, these are the PtC_2−H stretch, the PtC−CH stretch, the Pt−C_2H stretch, and then the two bend frequencies. The $^2\Pi$ state is Renner−Teller active; both bend components are included for both modes.

the $^3\Delta_g-{}^2\Delta_g$ transition based on the calculated parameters is nearly vertical (a slight activation of the in-phase HC−CNiC−CH stretch is predicted, and is within the signal observed). The $^3\Pi_g(2)-{}^2\Sigma^+$ transition is the most likely assignment for the low-intensity structure observed at 2.785(5) eV, while the lower intensity peaks just to the red of $^3\Delta_g(3)-{}^2\Delta_g(5/2)$ [2.944(7) eV] may then be due to $^3\Delta_g(2)-{}^2\Delta_g(3/2)$, which gives a 1400(70) cm^{-1} spin−orbit splitting in the anion. The $^3\Phi_g-{}^2\Delta_g$ transition is predicted to lie at an unperturbed energy of 3.47 eV, above the experimental cutoff.

PdC_2H^-. The broad and congested PE spectrum of PdC_2H^- (Figure 2, third panel) has been discussed in detail previously. The calculations on the anion and neutral, summarized in Table 6, support the original assignment of the spectral origin (Figure 2c, dotted trace) to the $^2\Sigma^+[...(1\delta)^4(2\pi)^4(4\sigma)]-{}^1\Sigma^+[...(1\delta)^4(2\pi)^4(4\sigma)^2]$ transition. The calculated EA is 2.01 eV, which agrees with the observed EA, 1.98(3) eV. The triplet manifold of PdC_2H^- lies above 1.1 eV, so these anion states were not pursued further. Two stable neutral states, $^2\Pi[...(1\delta)^4(2\pi)^3(4\sigma)^2]$ and $^2\Delta[...(1\delta)^3(2\pi)^4(4\sigma)^2]$, were also calculated to lie within 0.9 eV of the ground neutral state, and in principle could be observed in the spectrum.

The spin−orbit splitting in the $^2\Pi$ and $^2\Delta$ states should be on the order of several thousand wavenumbers (the splitting between the $^5/_2$ and $^3/_2$ components of the ^{2}D ground state of Pd^+ is 3539 cm^{-1})[31] so transitions to individual spin−orbit components of these states should be very well resolved. All three transitions are predicted to have some activation of the Pd−C_2H stretch, with the $^2\Delta-{}^1\Sigma^+$ expressing the most. There is an obvious mismatching of the experimental spectral profile with the calculated profiles. Since the anions were formed in a gas-phase reaction that may have been very exothermic, enormous vibrational temperatures may account for the disagreement in the breadth of band X. However, we cannot account for band A. No other PE spectrum in this series has broad, unresolved structure. The explanation may be a simple one involving thermionic emission, which is consistent with the lack of angular dependence in the signal of band A.

PtC_2H^-. The calculations on PtC_2H^- and PtC_2H, summarized in Table 7, predict a $^1\Sigma^+[...(1\delta)^4(2\pi)^4(4\sigma)^2]$ anion ground state and a $^2\Sigma^+[...(1\delta)^4(2\pi)^4(4\sigma)]$ neutral ground state with low-lying $^2\Delta[...(1\delta)^3(2\pi)^4(4\sigma)^2]$ and $^2\Pi[...(1\delta)^4(2\pi)^3(4\sigma)^2]$ states, analogous to the various states predicted for PdC_2H, PdCN and PtCN. The calculated EA is 2.70 eV, assuming the $^2\Sigma^+$ state lies below the perturbed spin−orbit components of the $^2\Delta$ and $^2\Pi$ states. The origin of the PtC_2H^- spectrum lies at 2.650(7) eV, which is in good agreement with the calculated EA. Excited states are predicted to lie within 0.15 eV of the ground neutral state. No additional distinct structure is observed in the spectrum within this energy window, even though transitions to these states are predicted to be nearly vertical.

IV. Discussion

There are a number of points of comparison between the electronic structures of the Ni, Pd, and Pt cyanide and acetylide complexes, and surface plots of several valence orbitals of these and related complexes, along with the orbital occupancies are shown in Figures 3−5 to facilitate discussion on this.

The reactions that produce these complexes are worth a brief comment. For the cyanides, large quantities of CN^- and the presence of $MCN_{n>1}^-$ suggests cyanide complexes form by simple association between the neutral metal atom and CN^- rather than by any direct reaction with acetonitrile. The formation of PdC_2H^- has been justified previously[18] as being from the $Pd + C_2H_3^- \rightarrow PdC_2H^- + H_2$ reaction, suggesting a similar reaction for PtC_2H^- formation. Both Pd ($4d^{10}$) and Pt ($6s5d^9$) have an s-orbital vacancy in their ground electronic states, which has been predicted to be a determining factor in metal atom reactivity.[32] No spontaneous reaction was observed between Ni and C_2H_4 or its radical anions. However, large quantities of $HNiC_2H^-$ and $Ni(C_2H)_2^-$ were observed when the ethylene was present at the ablation, so an excited state of Ni^- or Ni may be involved in the reaction. The mechanism for $Ni(C_2H)_2^-$ formation is likely to be very complicated, and we will not speculate on it further.

A striking feature that emerges from the DFT calculations on the cyanides that the ground state of NiCN is triplet (lowest singlet state at $T_e = 0.14$ eV) while the Pd and Pt analogues are singlet (triplet manifold at $T_e > 1$ eV). The same type of trend is observed in the nickel acetylide complexes in that the triplet neutrals (similar electronic structure to the anions of the other species) are more stable than the singlets. So, there is a stabilization of the 5σ orbital (shown in Figure 3) relative to

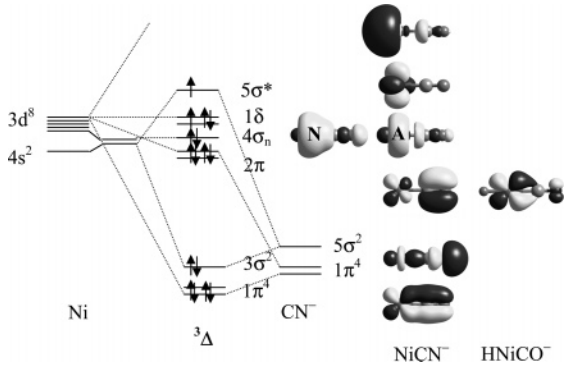

Figure 3. Molecular orbital diagram for NiCN/NiCN$^-$ showing the orbital occupancy of the $^3\Delta$ anion ground state. Surface plots of the NiCN$^-$ orbitals from the calculations are included, along with the 2π orbital of HNiCO for comparison.[20]

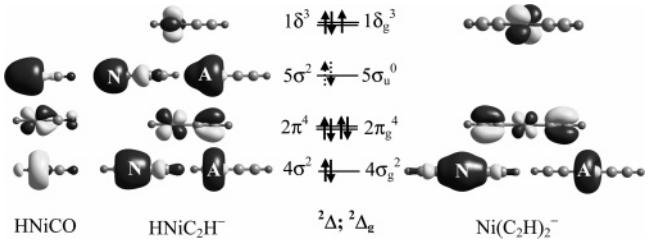

Figure 4. Valence orbitals of HNiC$_2$H/HNiC$_2$H$^-$ and Ni(C$_2$H)$_2$/Ni(C$_2$H)$_2^-$ showing the oribital occupancies of the anion ground states [$^3\Delta$ for HNiC$_2$H$^-$ and $^3\Delta_g$ for Ni(C$_2$H)$_2^-$]. Also included for comparison are several valence orbitals of HNiCO,[20] which is isoelectronic with HNiC$_2$H$^-$.

the other valence orbitals in the nickel complexes that does not occur in the heavier complexes.

Along the nickel complex series, we can loosely compare NiCN$^-$ and HNiC$_2$H, since they have the same number of valence electrons. Indeed, these two molecules share a $^3\Delta$ ground state. HNiC$_2$H$^-$ is isoelectronic with HNiCO, and these molecules share a $^2\Delta$ ground state,[20] though the ordering of the excited states are reversed. There is a fundamental difference in the 2π orbitals of HNiCO and HNiC$_2$H illustrated in Figure 4. For HNiCO/HNiCO$^-$, it is bonding between the Ni d_π orbital and the $2\pi_{CO}$* orbital (classic π back-donation) while in HNiC$_2$H/HNiC$_2$H$^-$ (and *all* the acetylide complexes here) the 2π orbital is the antibonding combination of Ni d_π and $1\pi_C$2H or CN.

Ni(C$_2$H)$_2$ differs from HNiC$_2$H in that it has a lower-lying nonbonding MO from the out-of-phase combination of the σ_n orbitals on the two C$_2$H ligands that essentially reduces the number of electrons localized on the nickel atom (dashed electrons in Figure 4 represent occupancy for HNiC$_2$H, vacancy for Ni(C$_2$H)$_2^-$).

The differences between the Pd and Pt series are more subtle. Orbitals and occupancies are shown in Figure 5. PtCN and PtC$_2$H are distinguished from the Pd complexes by the difference in the 4σ orbital. In Pt complexes, it is perfectly nonbonding and shows no obvious p_z hybridization, both of which are in contrast with Pd complexes (and NiCN). This, again, reflects the higher energy cost of *n*s−*n*p hybridization as *n* gets larger due to greater relativistic effects.[33] The anions of the palladium and platinum cyanides and acetylides are isoelectronic with PdCO and PtCO, all of which share the $^1\Sigma^+$ ground state.[20] Note again that there is a fundamental difference between the 2π orbitals of the carbonyls and the cyanides and acetylides. On the basis of the relative M−C and C═C or C≡N bond lengths and vibrational frequencies between the anion and neutral

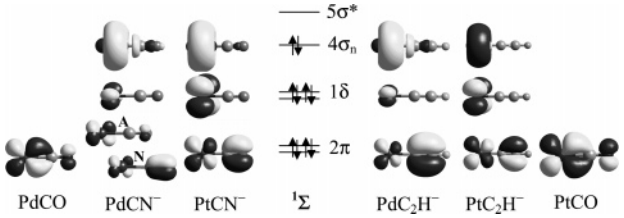

Figure 5. Three highest valence orbitals for PdCN/PdCN$^-$, PtCN/PtCN$^-$, PdC$_2$H/PdC$_2$H$^-$, and PtC$_2$H/PtC$_2$H$^-$ with the common, $^1\Sigma^+$ anion ground-state orbital occupancy shown. Also included for comparison is the 2π orbital of PdCO,[20] which is isoelectronic with the metal cyanide and acetylide ions.

complexes, there is some contribution from π* back-donation in the bonding of all cyanide and acetylide complexes. This effect is more pronounced in Pt vs Pd, and C$_2$H vs CN. That is, the PtC$_2$H complex appears to have the largest contribution from back-donation, and PdCN has the least. Put another way, the PdCN is the most ionic and PtC$_2$H is the least ionic, which is consistent when the relative EA's of the ligands and metals, along with the ionization potentials (IP) of the metals are taken into account (EA$_{CN}$ = 3.862(4) eV;[34] EA$_{C2H}$ = 2.969(6) eV;[35] EA$_{Pd}$ = 0.562(5),[36] EA$_{Pt}$ = 2.128(2);[37] IP$_{Pd}$ = 8.338 eV[38] and IP$_{Pt}$ = 8.959 eV[39]).

Overall, the calculated EAs and structures for these complexes were generally in good agreement with the observed spectral information. For PdCN, PtCN, PdC$_2$H, and PtC$_2$H, the calculated EAs were within 0.05 eV of the observed value. Except for PdC$_2$H$^-$, for which we believe the data analysis may have been confounded by extreme ion temperatures, the spectral profiles simulated using calculated parameters matched well. For NiCN, the calculated EA was off by considerably more (0.21 eV) than for the other species. The spin−orbit splitting in the anion and neutral should be on the same order of magnitude, so they should not result in an observed EA that deviates by this much from the calculated values. In the case of Ni(C$_2$H)$_2^-$, the first allowed transition from the ground anion state is an excited state, and the term energies of the excited states are somewhat less reliable than the ground-state energies.

V. Conclusions

The 3.49 eV PE spectra of NiCN$^-$, PdCN$^-$, PtCN$^-$, HNiC$_2$H$^-$, Ni(C$_2$H)$_2^-$, PdC$_2$H$^-$, and PtC$_2$H$^-$ have been interpreted by comparison with new DFT calculations on the neutral and anion ground and low-lying electronic states. The calculations predict linear structures for the ground anion and neutral states of all the complexes, and nearly linear states for several of the HNiC$_2$H and PtC$_2$H excited states. For PdCN, PtCN, PdC$_2$H, and PtC$_2$H, $^1\Sigma^+$ anion ground states (triplet manifolds lying above 1 eV) and $^2\Sigma^+$ neutral ground states are predicted. The nickel complexes were distinguished from the palladium and platinum complexes by the relative stability of the 5σ orbital, allowing higher spin states in the nickel complexes to be more stable. NiCN$^-$ and HNiC$_2$H have $^3\Delta$ ground states, and Ni(C$_2$H)$_2$ has a $^3\Pi$ ground state. NiCN, HNiC$_2$H$^-$, and Ni(C$_2$H)$_2^-$ all have $^2\Delta$ ground states. The structure observed in the spectra were generally very consistent with the calculated parameters, including EAs and vibrational profiles. Except for NiCN$^-$, the electronic transitions observed tended to be nearly vertical. Spin−orbit effects were not included in the calculations, though spin−orbit splitting in neutral states was directly observed in the spectra of HNiC$_2$H$^-$ and Ni(C$_2$H)$_2^-$.

Acknowledgment. C.C.J. gratefully acknowledges support from NSF CHE-9875046 and ARO DAAD 19-03-1-0009.

References and Notes

(1) Negishi, E.; Anastasia, L. *Chem. Rev.* **2003**, *103*, 1979.
(2) Percec, V.; Hill, D. H. *ACS Symp. Ser.* **1996**, *624*, 2.
(3) Serra, G.; Chaudret, B.; Saillard, Y.; Lebeuze, A.; Rabaa, H.; Ristorcelli, I.; Klotz, A *Astron. Astrophys.* **1992**, *260*, 489.
(4) Sharpe, A. G. *The chemistry of cyano complexes of the transition metals*; Academic Press: London, 1976.
(5) Dunbar, K. R.; Heintz, R. A. *Prog. Inorg. Chem.* **1997**, *45*, 283.
(6) Kingston, C. T.; Merer, A. J.; Varberg, T. D. *J. Mol. Spectrosc.* **2002**, *215*, 106.
(7) Heath, J. R.; Ratner, M. A. *Phys. Today* **2003**, *56*, 43.
(8) For example, Morrall, J. P.; Powell, C. E.; Stranger, R.; Cifuentes, M. P.; Humphrey, M. G.; Heath, G. A. *J. Organomet. Chem.* **2003**, *670*, 248.
(9) Verbist, T.; Houbrechts, S.; Kauranen, M.; Clays, K.; Persoons, A. *J. Mater. Chem.* **1997**, *7*, 2175.
(10) Yam, V. W.-W. *Acc. Chem. Res.* **2002**, *35*, 555.
(11) (a) Michalak, A.; Ziegler, T. *Organomet.* **2003**, *22*, 2069. (b) *ibid*, *Macromol.* **2003**, *36*, 929.
(12) Britovsek, G. J.; Baugh, S. P. D.; Hoarau, O.; Gibson, V. C.; Wass, D. F.; White, A. J. P.; Williams, D. J. *Inorg. Chim. Acta* **2003**, *345*, 279.
(13) Leatherman, M. D.; Svejda, S. A.; Johnson, L. K.; Brookhart, M. *J. Am. Chem. Soc.* **2003**, *125*, 3068.
(14) Douglas, O.; Brookhart, M. *Organometallics* **2002**, *21*, 5926.
(15) Judai, K.; Abbet, S.; Worz, A. S.; Ferrari, A. M.; Giordano, L.; Pacchioni, G.; Heiz, U. *J. Mol. Catal. A: Chem.* **2003**, *199*, 103.
(16) Medlin, J. W.; Allendorf, M. D. *J. Phys. Chem. B* **2003**, *107*, 217.
(17) Sheh, P. A.; Neurock, M.; Smith, C. M. *J. Phys. Chem. B* **2003**, *107*, 2009.
(18) Moravec, V. D.; Jarrold, C. C. *J. Chem. Phys.* **2000**, *112*, 792.
(19) Klopcic, S. A.; Moravec, V. D.; Jarrold, C. C. *J. Chem. Phys.* **1999**, *110*, 8986.
(20) Chatterjee, B.; Akin, F. A.; Jarrold, C. C.; Raghavachari, K. *J. Chem. Phys.* **2003**, *119*, 10591.
(21) Akin, F. A.; Jarrold, C. C. *J. Chem. Phys.* **2003**, *118*, 1773.
(22) Gaussian 98, Revision A.9. Frisch, M. J.; et al. Gaussian: Pittsburgh, PA 15213. Note that the 6-311+G basis set for Ni, as defined in Gaussian 98, is actually a (15s, 11p, 6d) basis set contracted to (10s, 7p, 4d).
(23) (a) Becke, A. D. *J. Chem. Phys.* **1993**, *98*, 5648. (b) Hohenberg, P.; Kohn, W. *Phys. Rev. B.* **1964**, *136*, 864. (c) Becke, A. D. *Phys. Rev. A* **1988**, *38*, 3098. (d) Vosko, S. H.; Wilk, L.; Nusair, M. *Can. J. Phys.* **1980**, *58*, 1200. (e) Lee, C.; Yang, W.; Parr, R. G. *Phys. Rev. B* **1988**, *37*, 785. (f) Miehlich, B.; Savin, A.; Stoll, H.; Preuss, H. *Chem. Phys. Lett.* **1989**, *157*, 200.
(24) Shenstone, A. G. *J. Res. Natl. Bur. Stand. (U.S.)* **1970**, *74A*, 801.
(25) Moravec, V. D.; Klopcic, S. A.; Jarrold, C. C. *J. Chem. Phys.* **1999**, *110*, 5079.
(26) The splitting between the $J = {}^5/_2$ and ${}^3/_2$ levels of the ground ^{2}D-($5d^9$) state of Pt^+ is 8419 cm^{-1} (1.044 eV), per: Blaise, J.; Wyart, J.-F. *J. Res. Natl. Inst. Stand. Technol. (U.S.)* **1992**, *97*, 217.
(27) Cooper, J.; Zare, R. N. *J. Chem. Phys.* **1968**, *48*, 942.
(28) Litzén, U.; Lundberg, H.; Tchang-Brillet, W.-U. L.; Launay, F.; Engleman, R., Jr. *Phys. Scr.* **2001**, *64*, 63.
(29) For instance: Wittborn, A. M. C.; Costas, M.; Blomberg, M. R. A.; Siegbahn, P. E. M. *J. Chem. Phys.* **1997**, *107*, 4318.
(30) Balasubramanian, K. *J. Phys. Chem.* **1989**, *93*, 6585.
(31) Bradforth, S. E.; Kim, E. H.; Arnold, D. W.; Neumark, D. M. *J. Chem. Phys.* **1993**, *98*, 800.
(32) Ervin, K. M.; Lineberger, W. C. *J. Phys. Chem.* **1991**, *95*, 1167.
(33) Ho, J.; Ervin, K. M.; Polak, M. L.; Gilles, M. K.; Lineberger, W. C. *J. Chem. Phys.* **1991**, *95*, 4845.
(34) Hotop, H.; Lineberger, W, C. *J. Phys. Chem. Ref. Data* **1985**, *14*, 731.
(35) Callender, C. L.; Hackett, P. A.; Rayner, D. *J. Opt. Soc. Am. B* **1988**, *5*, 614.
(36) Marijnissen, A.; ter Meulen, J. J.; Hackett, P. A.; Simard, B. *Phys. Rev. A* **1995**, *52*, 2606.